Design of isomorphic symmetric descendants of the Miura-ori

2015 Smart Mater. Struct. 24 085001

(http://iopscience.iop.org/0964-1726/24/8/085001)

IOP Publishing Smart Materials and Structures
Smart Mater. Struct. **24** (2015) 085001 (12pp) doi:10.1088/0964-1726/24/8/085001

Design of isomorphic symmetric descendants of the Miura-ori

Pooya Sareh and Simon D Guest

University of Cambridge, UK

E-mail: p.sareh@imperial.ac.uk

Received 8 March 2015, revised 17 May 2015
Accepted for publication 19 May 2015
Published 30 June 2015

Abstract

The Miura-ori is a classic flat-foldable tessellation which has its root in origami, but has been applied to the folding of reconfigurable structures for a variety of engineering and architectural applications. In recent years, researchers have introduced design variations on the Miura-ori which change both the form and the function of the pattern. This paper introduces the family of isomorphically generalized symmetric variations of the Miura-ori. We study the Miura crease pattern as a wallpaper pattern. We reduce the symmetry of the original crease pattern to design new patterns while at the same time preserving the symmetry group of the tessellation as well as the flat-foldability condition at each node. It will be shown that—through appropriate design variations on the original pattern—we are able to use the Miura-ori to design either globally planar, or globally curved, flat-foldable patterns.

Keywords: origami, the Miura-ori, flat-foldability, symmetry, wallpaper groups

(Some figures may appear in colour only in the online journal)

1. Introduction

The Miura fold pattern, or the Miura-ori [1], is a flat-foldable origami tessellation with various engineering and architectural applications. From a symmetry standpoint, the Miura-ori is a tessellation with *pmg* symmetry (in the international notation [2]), which is one of the seventeen *plane symmetry groups* or *wallpaper groups*. It has been shown (see, e.g., [3]) that there are exactly seventeen distinct wallpaper groups. Every wallpaper pattern has a finite region called a *unit cell* which repeats under the action of two linearly independent translations. Each group has a unique unit cell which includes a certain number of *symmetry elements*, placed in certain positions relative to the unit cell. The symmetry elements include centres of *rotation*, axes of *reflection*, and axes of *glide reflection*. Schattschneider [4] presents the international notation for the seventeen plane symmetry groups. Two wallpaper patterns are said to be *isomorphic* if they belong to the same symmetry group, although they may have different unit cells.

Various scholars have presented design variations on the Miura-ori which change both the form and the function of the pattern (see, e.g., [5] or [6]). The authors of this paper have already developed a framework for the symmetric generalization of the Miura-ori [7]. In this paper, we briefly present the basic concepts and definitions underlying the framework which are necessary to understand the design process of the isomorphic descendants of the Miura-ori. In the framework there are two general assumptions that we use throughout this study. Firstly, we consider a crease pattern to be a set of *directionless* creases. In other words, the *fold direction* or *mountain-valley assignment* of fold lines does not affect the symmetry of a pattern. Secondly, two crease patterns are considered to be *similar* if a uniform scaling or rigid motion of one of them can make it coincide with the other one. A variation on a given Miura fold pattern is considered to be a *legitimate variation* if the following requirements are met: (1) all facets remain convex quadrilaterals; (2) the *global zigzag* condition (see [7] for an explanation of this concept) of the pattern is preserved.

There are two different choices for the unit cell which both match the standard *pmg* unit cell used in the International Tables for Crystallography [2], as depicted in figure 1. We primarily use the unit cell shown on the top of the figure along with its axes, throughout this work. We call this the *primary standard* choice for the smallest unit cell of the

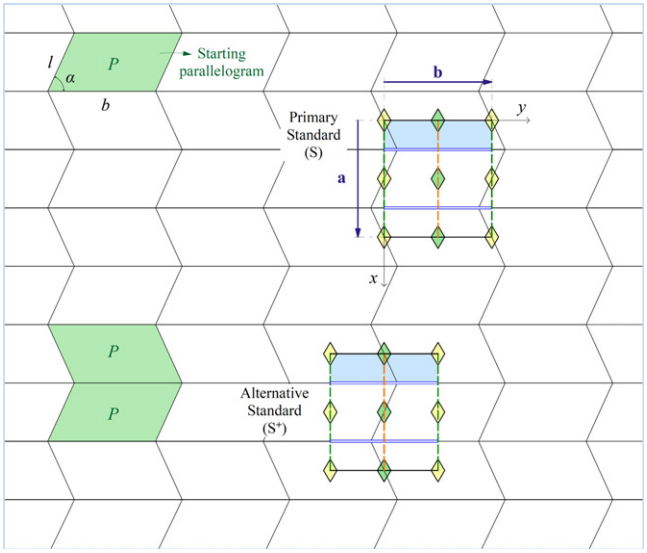

Figure 1. Two standard choices for the smallest *pmg* unit cell for the Miura-ori. Double and dashed lines represent reflection and glide reflection axes, respectively. 2-fold axes are shown by rhombuses. The blue shaded area shows the fundamental region of the pattern. The starting parallelogram of the pattern is shaded in green. The unit fragment of the pattern consists of a pair of starting parallelograms, as depicted on the bottom left of the figure.

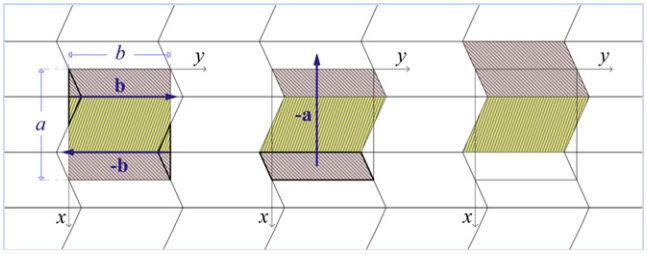

Figure 2. Recomposition of the Miura-ori unit cell to form its unit fragment.

Miura-ori. However, in order to cover a wider range of variations, it is necessary to consider an *alternative standard* choice for the smallest unit cell of the Miura-ori, which is marked by a '+' symbol. The blue shaded area shows the *fundamental region* of the pattern. A fundamental region is a minimal part of a pattern that generates the entire pattern under the action of all the symmetry operators which exist in the pattern [8]. Different colours for a symmetry element represent different classes of that element in the pattern. Note that the entire pattern can be generated from a unit cell by only translations. The translation vectors of the pattern in the x- and y-directions are shown as **a** and **b**, respectively. For a typical Miura-ori crease pattern shown in figure 1, the 'starting parallelogram' of the pattern, P, from which the entire pattern can be generated by symmetry operations, is shaded in green. It has an acute angle α, and two side lengths b and l, where b is along the horizontal lines of the pattern, i.e. along the y-direction. We define a *unit*

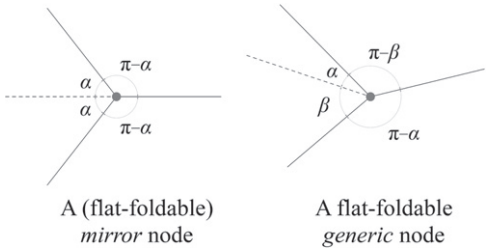

Figure 3. A (flat-foldable) mirror node versus a flat-foldable generic node.

fragment of a repetitive mesh to be a collection of adjacent facets which generate the entire pattern using the translation vectors of the pattern. The unit fragment of the Miura fold pattern, as depicted on the bottom left of figure 1, consists of a pair of starting parallelograms which share a fold line on the horizontal lines of the pattern, i.e. along the y-direction.

The unit cell of a repetitive mesh can be recomposed to obtain its unit fragment [7]. From figure 2 we can see that the smallest unit cell of the Miura-ori contains two parallelograms. The left hand section of this figure shows how to move the triangular fragments (bordered by bold lines) formed by the crease lines and the borders of the unit cell to obtain the figure in the middle; it is then sufficient to translate the bordered parallelogram on the bottom of the middle figure in the opposite x-direction to form two complete parallelograms. We use this recomposition process to find out the number of quadrilaterals within the unit cell of a crease pattern throughout this study.

The recomposition process gives us the number of quadrilaterals 'in each direction' in the unit cell of a pattern. As figure 2 shows, the smallest unit cell for the Miura-ori contains two parallelograms in the x-direction and one parallelogram in the y-direction. We call this crease pattern a $pmg_{2,1}$ pattern. We classify the crease patterns obtained by applying variations on the Miura fold pattern using the following definition:

Definition 1. A repetitive convex quadrilateral mesh designed by displacing the nodes of the Miura fold pattern is called $G_{i,j}$, where G is the name of its maximal plane symmetry group, and i and j are the number of quadrilaterals in the x- and y-directions, respectively, within the unit cell of the pattern. The y-direction is the direction of the parallel fold lines in the Miura fold pattern before applying variations. Variations of the Miura-ori which can only be designed based on the alternative unit cell (shown in figure 1) are denoted by $G^{+}_{i,j}$.

The Miura fold pattern consists of only one node type which is flat-foldable for any fold angle α_0 ($\alpha_0 \neq 0$ or π). We call this node type a *mirror node*. A degree-4 node which is not a mirror node is called a *generic node*. Figure 3 shows a (flat-foldable) mirror node versus a flat-foldable generic node (note that opposite angles must sum to π in order for a node to be flat-foldable [9]).

In the next section, we study the isomorphic symmetric variations of the Miura-ori.

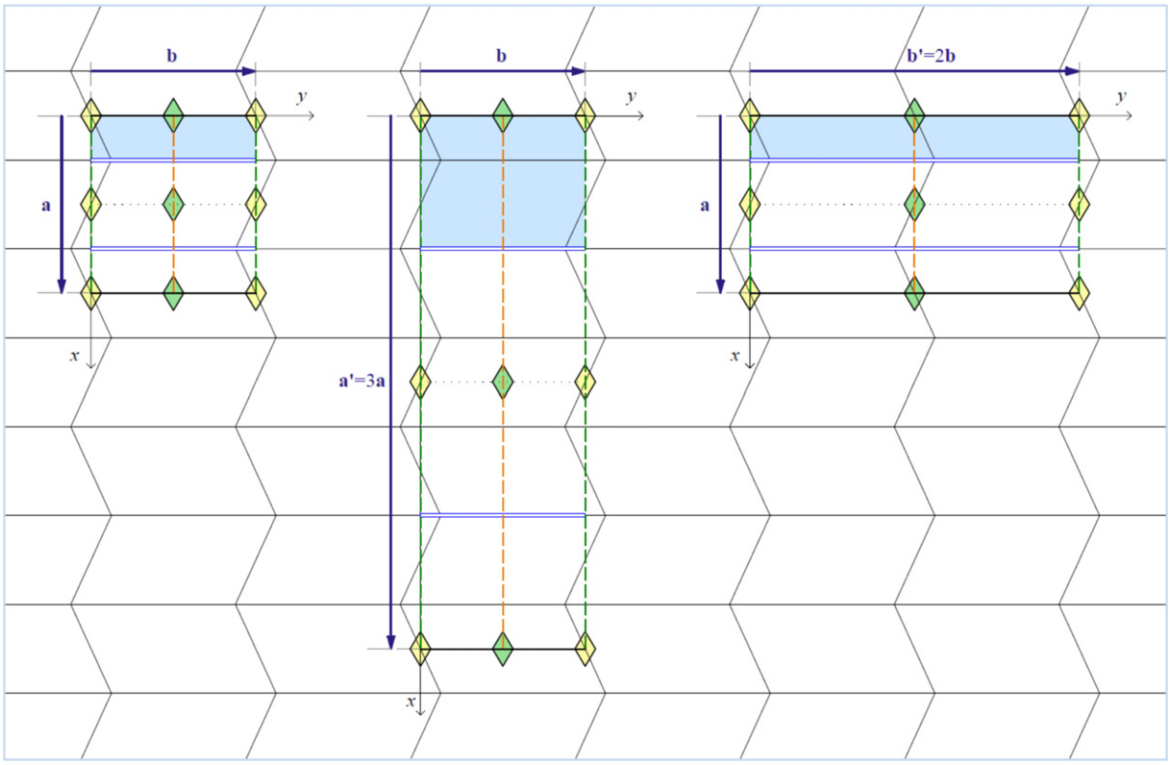

Figure 4. From left to right, the unit cells for $pmg_{2,1}$, $pmg_{6,1}$, and $pmg_{2,2}$.

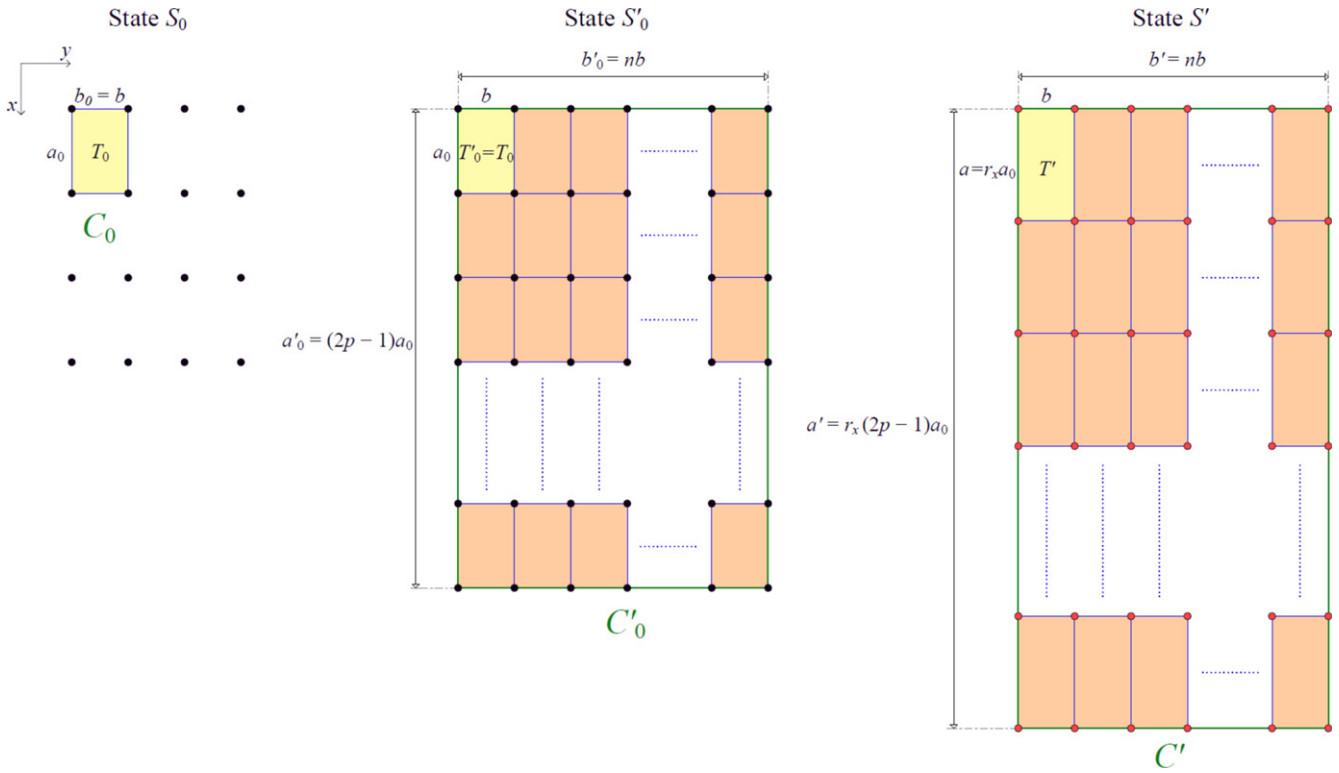

Figure 5. The unit cell of a *pmg* pattern in three different states. State S_0: the smallest unit cell C_0 based on a rectangular lattice of points. State S'_0: an enlarged unit cell, according to the scheme introduced earlier, based on the same lattice of points as in State S_0. State S': a unit cell with the same number of tiles in each direction as in State S'_0, but with a different height for the tile. It is based on a different rectangular lattice of points shown in red.

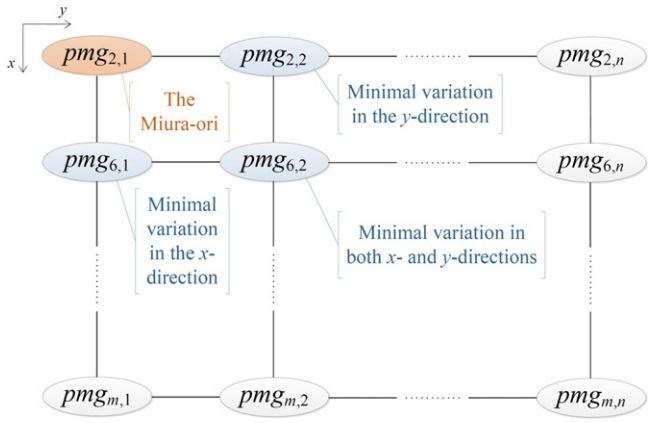

Figure 6. Unit cell growth scheme for isomorphic variations on the Miura-ori; the three minimal variations are highlighted in blue.

2. Isomorphic variations of the Miura-ori

Consider a *pmg* unit cell with lattice translation vectors **a** and **b**. According to the International Tables for Crystallography [2], the maximal isomorphic subgroup for this group has a unit cell with $\mathbf{a}' = 3\mathbf{a}$, or alternatively, a unit cell with $\mathbf{b}' = 2\mathbf{b}$. For a Miura fold pattern, these unit cells which are called $pmg_{6,1}$ and $pmg_{2,2}$ respectively, are depicted in figure 4 alongside the smallest possible unit cell, $pmg_{2,1}$.

A unit cell with $\mathbf{a}' = m\mathbf{a}$ defines an isomorphic subgroup of the initial unit cell provided that m is an odd number, while a unit cell with $\mathbf{b}' = n\mathbf{b}$ defines an isomorphic subgroup of the initial unit cell for any natural number n [2]. According to the discussion above, the symmetry group *pmg* allows us to expand the initial $pmg_{2,1}$ unit cell to a larger one of the form $pmg_{(4i-2),j}$, where i and j are natural numbers. Knowing this pattern for the growth of the unit cell, our goal is to investigate the possibility of preserving the flat-foldability condition of a crease pattern while enlarging its unit cell.

The unit cell variation scheme is illustrated in figure 5. State S_0 in this figure shows the rectangular lattice of points associated with a *pmg* wallpaper pattern, a Miura fold pattern in our case. It should be noted that these lattice points are different from the nodes (vertices) of the fold pattern. The yellow shaded rectangle is the smallest unit cell of the pattern, C_0, which is also called a *tile* T_0. It has a height a_0 and a width b_0. The *aspect ratio* of the unit cell can be expressed as:

$$\bar{a}_0 = \frac{a_0}{b_0}. \tag{1}$$

State S_0' shows the enlarged unit cell according to the enlargement scheme introduced earlier, while preserving the

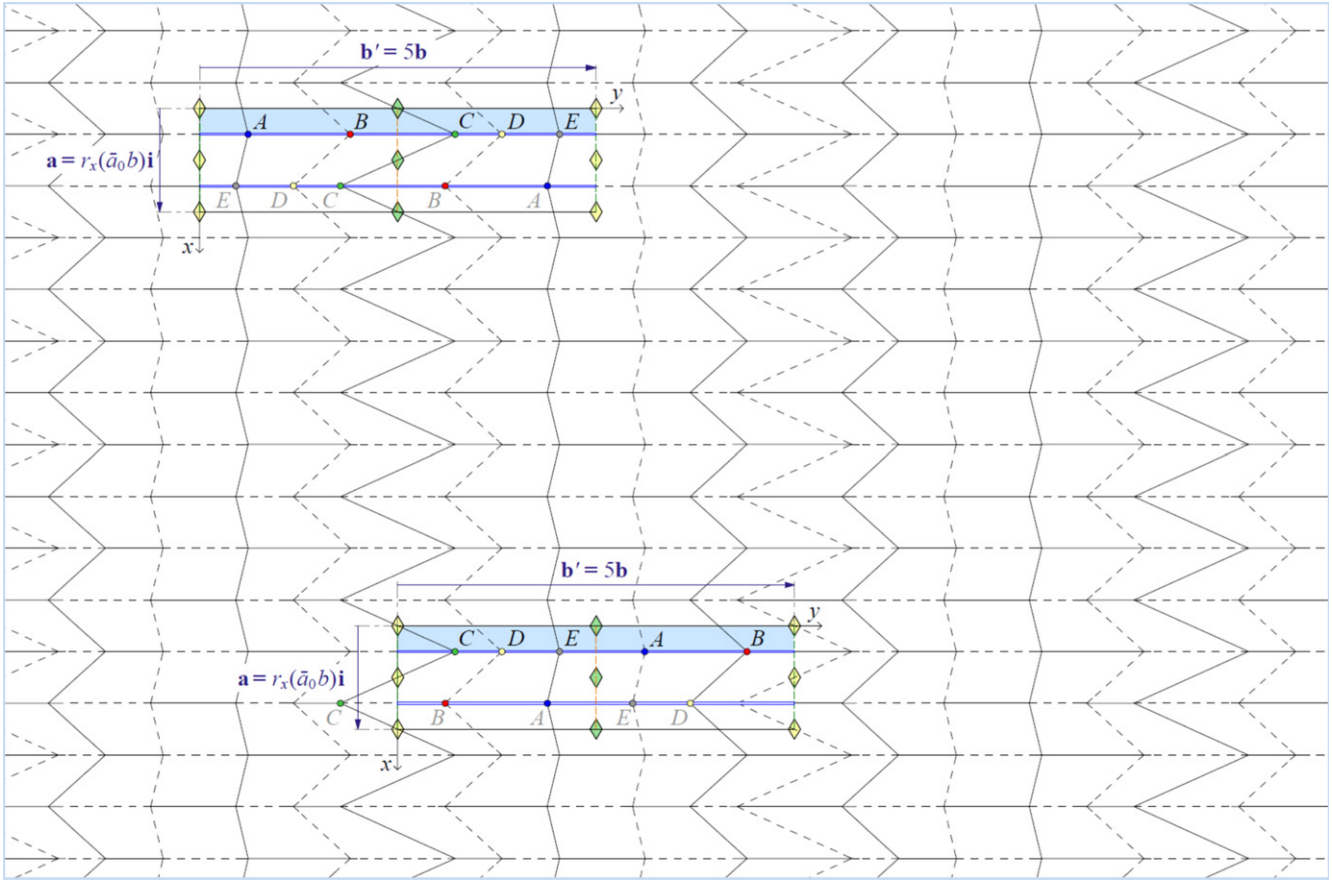

Figure 7. Upper unit cell: $pmg^{+}_{2,5}$; lower unit cell: $pmg_{2,5}$.

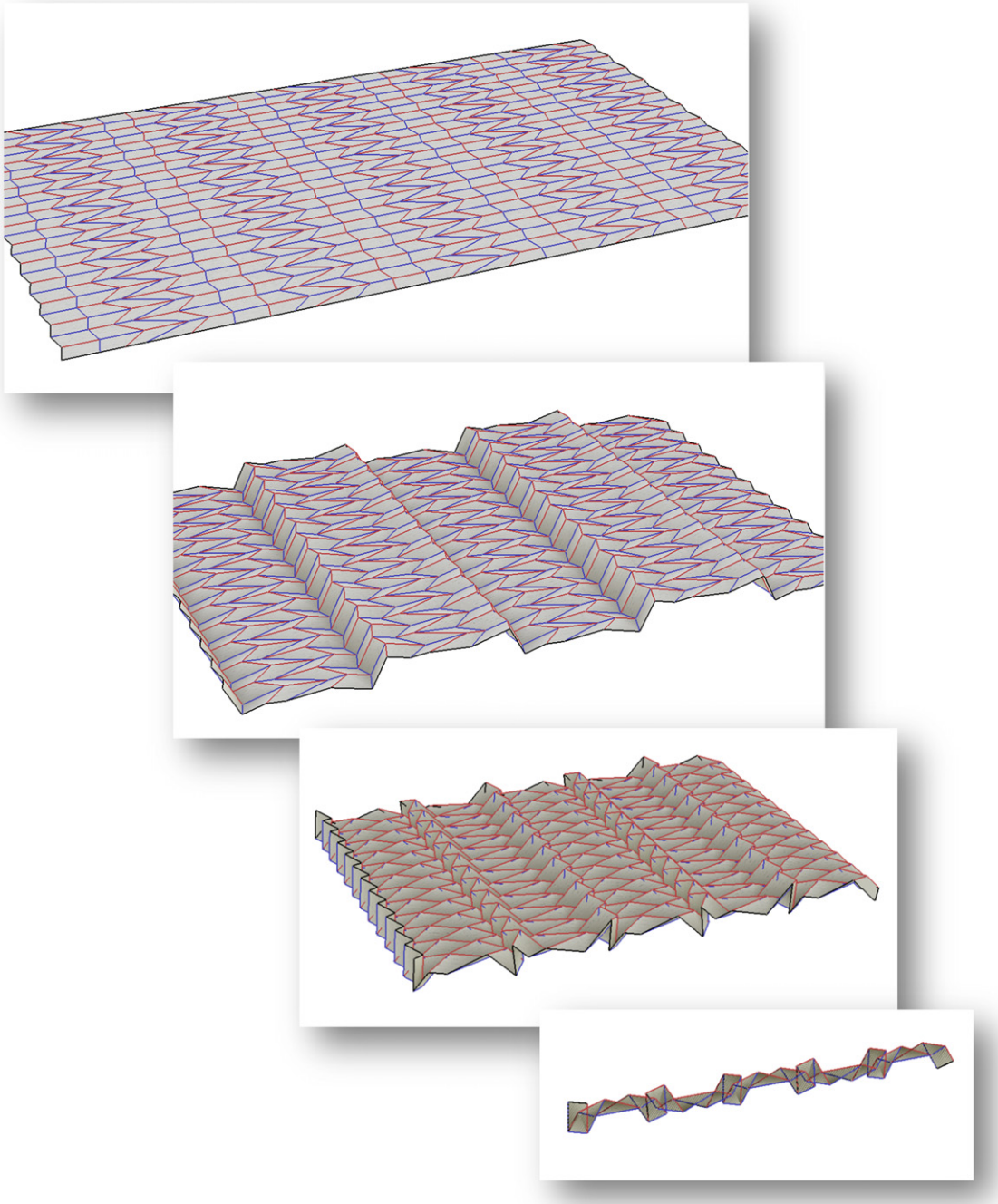

Figure 8. Simulation of the folding process of the $pmg_{2,5}$ pattern shown in the previous figure, using the Freeform Origami software [11].

same lattice of points. In fact, the transformation of the unit cell from C_0 to C_0' is a non-uniform scaling of C_0 with scale factors $2p-1$ and n in the x- and y-directions, respectively, where p and n are natural numbers.

After choosing a larger unit cell, C_0', we have a degree of freedom for changing the aspect ratio of the starting tile of the pattern, while retaining the same number of tiles in each direction. Without loss of generality, we can assume that the width of the unit cell remains unchanged, i.e.: $b = b_0$. For States S_0' and S' we have: $b' = b_0' = nb$. The aspect ratio of the unit cell for State S_0' is defined as follows:

$$\bar{a}_0' = \frac{a_0'}{b_0'} = \frac{(2p-1)a_0}{nb} = \frac{2p-1}{n}\bar{a}_0. \qquad (2)$$

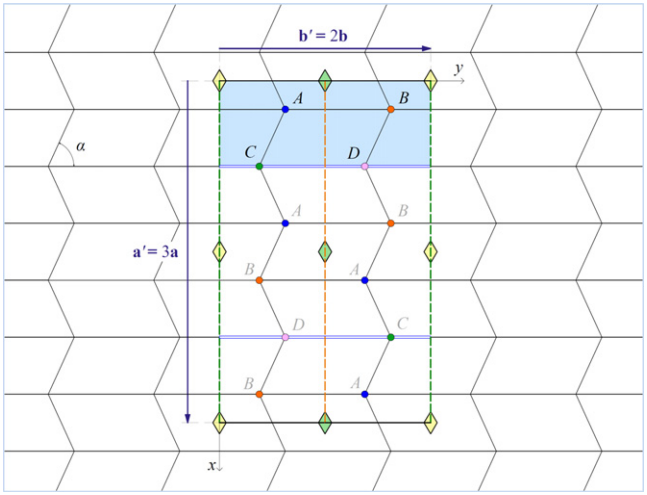

Figure 9. From a symmetry point of view, a $pmg^{+}_{6,2}$ unit cell contains four distinct orbits of nodes, shown as A, B, C and D.

Similarly, the aspect ratio of a variation of the Miura-ori, State S', is defined as following:

$$\bar{a}' = \frac{a'}{b'} = \frac{r_x a'_0}{r_y b'_0} = \frac{r_x}{r_y}\frac{2p-1}{n}\bar{a}_0, \tag{3}$$

where r_x and r_y are *scale factors* in the x- and y-directions, respectively. As we have already assumed that we do not change the width of the enlarged unit cell, i.e. $r_y = 1$, the *relative aspect ratio* of a variation of the Miura-ori to an initial Miura pattern with an aspect ratio $\bar{a}_0$ can be expressed as:

$$\frac{\bar{a}'}{\bar{a}_0} = \underbrace{\left(\frac{2p-1}{n}\right)}_{S_0 \to S'_0} \times \underbrace{r_x}_{S'_0 \to S'}, \tag{4}$$

where the first term of the product is the scale factor for the transformation from State S_0 to State S'_0, and the second term is the scale factor for the transformation from State S'_0 to State S'. The scale factor for the initial enlargement of the unit cell depends on the size of the unit cell which we choose on the original pattern on which we are making variations, and the second term of the product describes how to scale the height of the enlarged unit cell while preserving its width. The height of the final unit cell is as follows:

$$a' = r_x(2p-1)\bar{a}_0 b. \tag{5}$$

Figure 6 shows the unit cell growth scheme for isomorphic variations on the Miura-ori, where the three minimal variations are highlighted in blue. In the next section, we study the minimal isomorphic variations of the Miura-ori. Then we will investigate the problem for the isomorphically generalized case.

It can be shown that for a $G_{i,j}$ variation of the Miura-ori, if j is odd, $G_{i,j}$ and $G^{+}_{i,j}$ are the same, but if j is even, they are different patterns. This fact is revealed through an example pattern depicted in figure 7 [10]. In this figure, the pattern is generated by making variations on a $pmg^{+}_{2,5}$ unit cell, shown in the upper part of the figure. This can also be generated based on the $pmg_{2,5}$ unit cell shown in the lower part of the figure. Therefore, $pmg_{2,5}$ and $pmg^{+}_{2,5}$ are the same pattern. A computer simulation of the folding process of this pattern using the Freeform Origami software [11] is depicted in figure 8.

2.1. Minimal isomorphic symmetric variations

The two variations $pmg_{6,1}$ and $pmg_{2,2}$ are the *minimal isomorphic variations* of the Miura-ori in the x- and y-directions, respectively. $pmg_{6,2}$ is the first variation in which the unit cell has enlarged in both x- and y-directions in comparison to the smallest unit cell for the Miura-ori. In this sense, it is the minimally generalized variation of the Miura-ori in two directions. The derivations of the minimal variations of the Miura-ori have been presented in [12]. To avoid duplication, we refrain from repeating them in this paper. Here, as an example, we present the derivation of a novel pattern. Starting from the alternative standard unit cell, S^{+}, illustrated in figure 1, we can design a 6×2 isomorphic variation of the Miura-ori, $pmg^{+}_{6,2}$, which is different from $pmg_{6,2}$. A $pmg^{+}_{6,2}$ unit cell is illustrated in figure 9. There are four distinct *orbits* of nodes associated with the unit cell, shown as A, B, C and D (the position of every node in an orbit is defined by symmetry operations from the position of any one node within the orbit). As we are working with a *pmg* group, we have a degree of freedom for the aspect ratio of the unit cell. There are two degrees of freedom associated with the position of each of the two nodes A and B. Also there is one degree of freedom to move each of the nodes C and D along the mirror line—it is not, however, possible to move any of them in the x-direction within a fixed unit cell, as the reflection line restrains movements in this direction to retain the symmetry.

Figure 10 shows a Miura fold pattern in its original configuration, State (0); in the lower part of the figure, we have perturbed the pattern using all the degrees of freedom that we introduced earlier to obtain a new configuration, State (1). Note that State (1) is not flat-foldable in general; we present a flat-foldable variation of it later in this section.

In order to investigate the application of the flat-foldability condition to the pattern at nodes A and B, we have illustrated the fundamental region of a typical $pmg^{+}_{6,2}$ variation of the Miura-ori accompanied by its surrounding fold lines in figure 11. Indices l and r represent the neighbouring fundamental regions on the left and right side of the blue shaded fundamental region, respectively.

Applying the flat-foldability constraint at nodes A and B, respectively, we get:

$$\gamma_2 = \pi - \alpha, \tag{6}$$

$$\gamma_3 = \alpha. \tag{7}$$

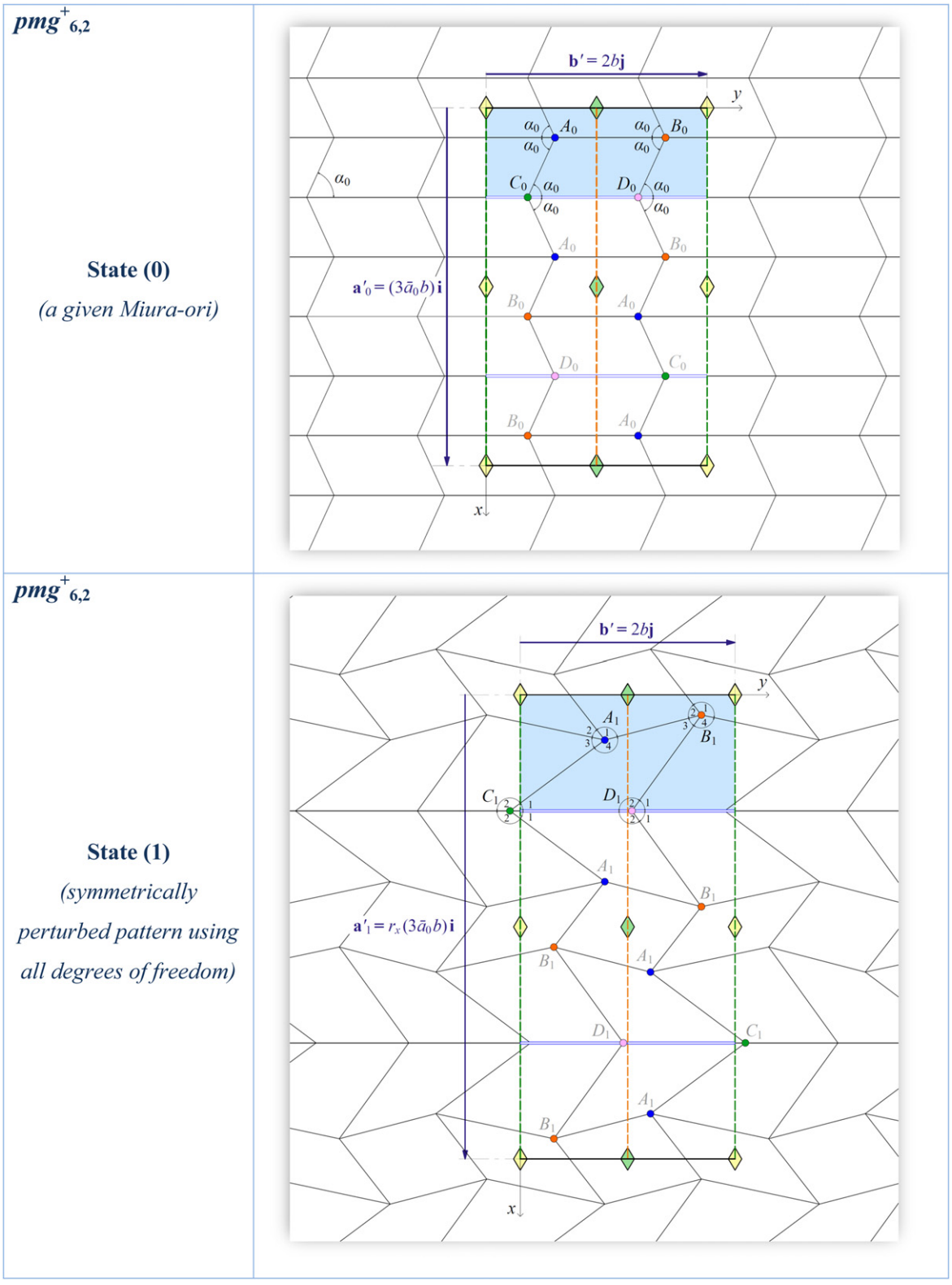

Figure 10. A $pmg^{+}_{6,2}$ variation of the Miura-ori. State (0): a given Miura fold pattern. State (1): a perturbed state using all degrees of freedom. State (1) is not flat-foldable in general; we present a flat-foldable variation of it later in this section.

From the two above equations we obtain:

$$\gamma_2 + \gamma_3 = \pi, \tag{8}$$

which implies that the two line segments AC and BD are parallel. Therefore, all transverse polylines in a flat-foldable $pmg^{+}_{6,2}$ variation of the Miura-ori must be piecewise parallel. In other words, all flat-foldable $pmg^{+}_{6,2}$ variations of the Miura-ori are globally planar (in contrast, we have shown that [12] the flat-foldable $pmg_{6,2}$ variations of the Miura-ori can be either globally planar, or globally curved. A simulation of the

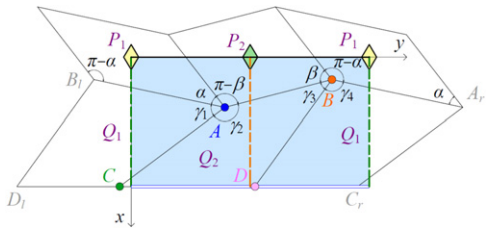

Figure 11. The fundamental region of a typical $pmg^{+}_{6,2}$ variation of the Miura-ori along with its surrounding crease lines. Indices l and r represent the neighbouring fundamental regions on the left and right side of the blue shaded fundamental region, respectively.

folding process of an example fold pattern [12] for the globally curved $pmg_{6,2}$ variations of the Miura-ori is depicted in figure 12). From the flat-foldability condition at nodes A and B we can also write:

$$\gamma_1 = \beta, \tag{9}$$

$$\lambda_4 = \pi - \beta. \tag{10}$$

From equations (6), (7), (9) and (10) we conclude that the two nodes A and B are geometrically congruent, i.e. $A \cong B$. There is a similar relationship between nodes C and D, i.e. $C \cong D$.

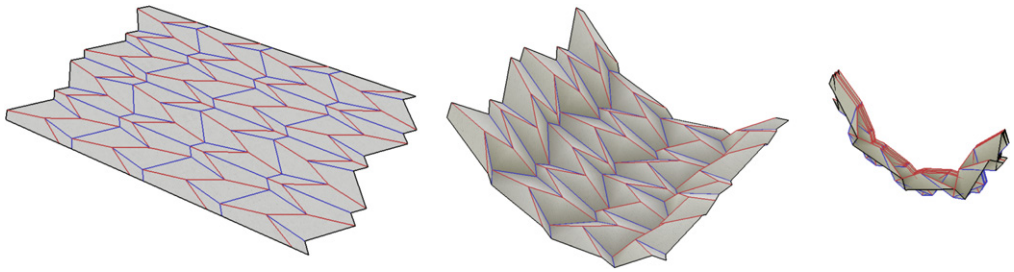

Figure 12. Simulation of the folding process of a globally curved $pmg_{6,2}$ variation of the Miura-ori using the Freeform Origami software [11].

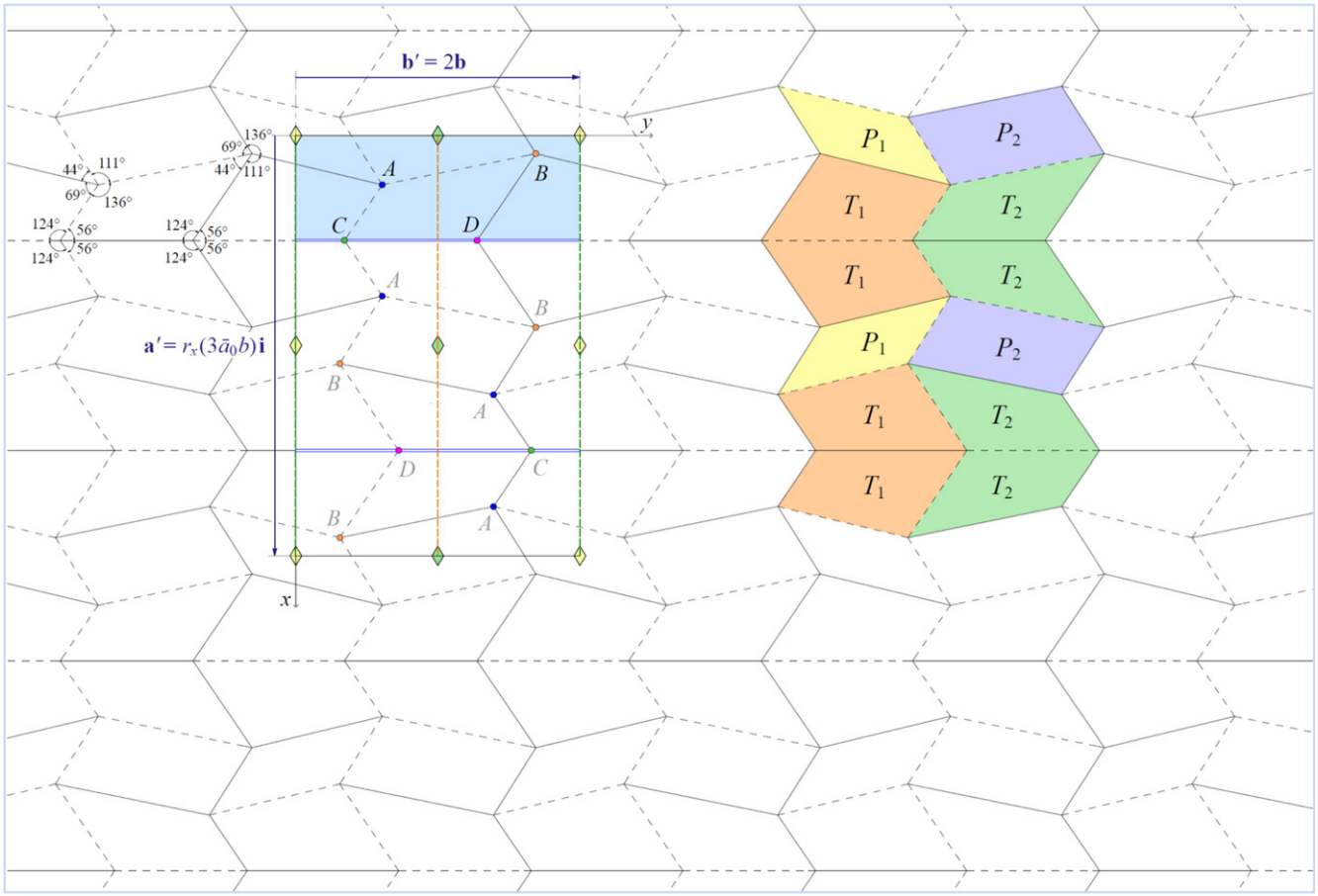

Figure 13. An example for a flat-foldable $pmg^{+}_{6,2}$ variation of the Miura-ori. It consists of two different starting parallelograms, shown as P_1 and P_2, as well as two different starting trapezoids, shown as T_1 and T_2 solid lines show mountain fold lines, while dashed lines represent valley fold lines.

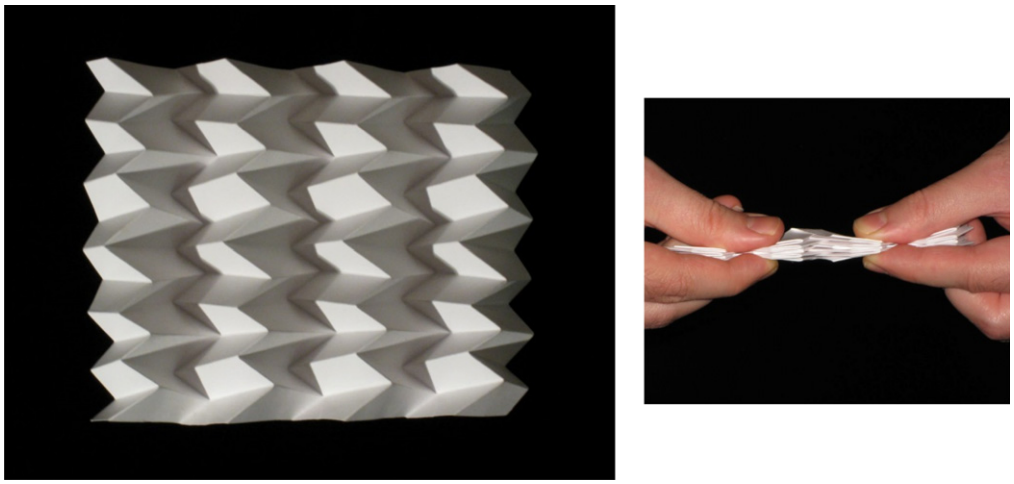

Figure 14. A cardboard model of the fold pattern depicted in the previous figure in a partially folded condition (left) and the flat-folded condition (right).

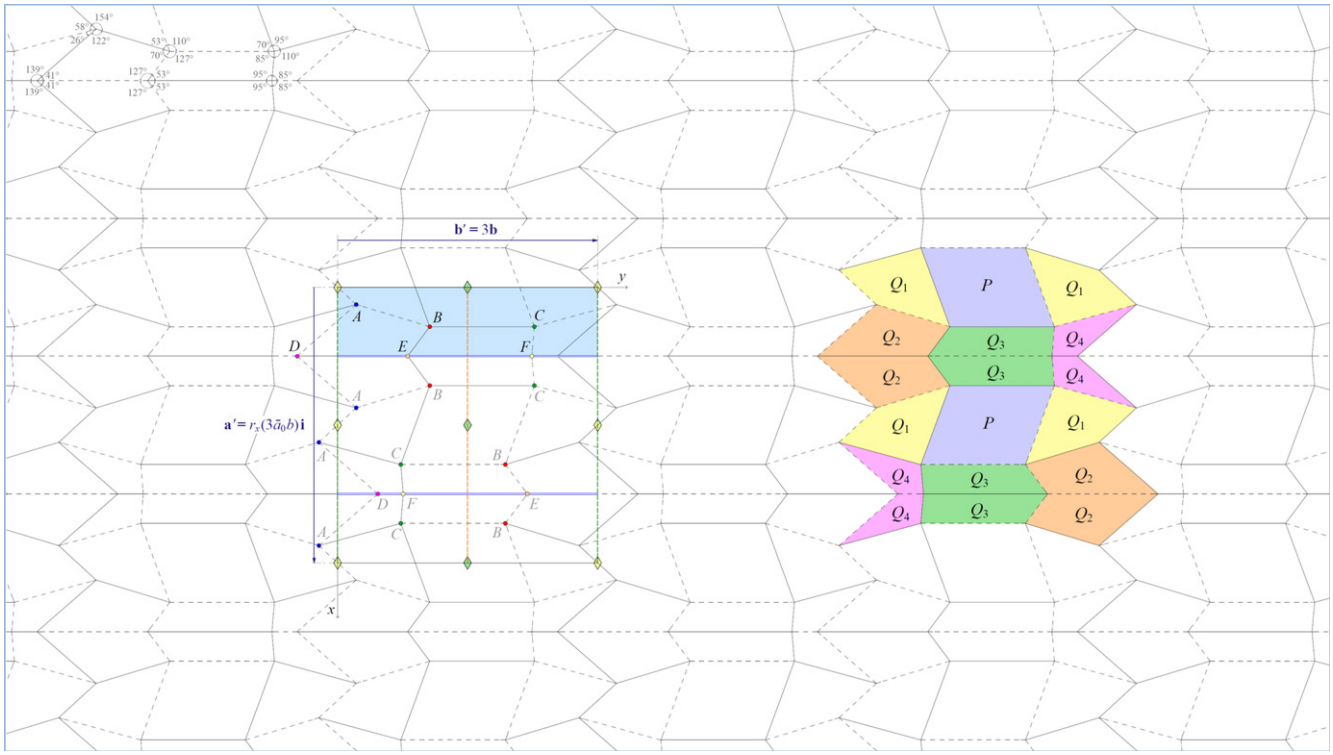

Figure 15. An example for a flat-foldable $pmg_{6,3}$ variation of the Miura-ori. It consists of four different starting convex quadrilaterals, shown as Q_1, Q_2, Q_3 and Q_4, as well as a single parallelogram. Solid lines show mountain fold lines, while dashed lines represent valley fold lines.

Figure 13 shows an example for a flat-foldable $pmg^{+}_{6,2}$ variation of the Miura fold pattern alongside the assigned mountains and valleys. The pattern consists of two different starting parallelograms, shown as P_1 and P_2, as well as two different starting trapezoids, shown as T_1 and T_2. Figure 14 shows a cardboard model of the fold pattern depicted in figure 13.

2.2. Generalized isomorphic symmetric variations

The generalization of the Miura-ori in both longitudinal and transverse directions simultaneously has the general form $pmg_{m,n}$, where $m = 2(2p - 1)$, and n and p are natural numbers. Depending on whether n is odd or even, the centre

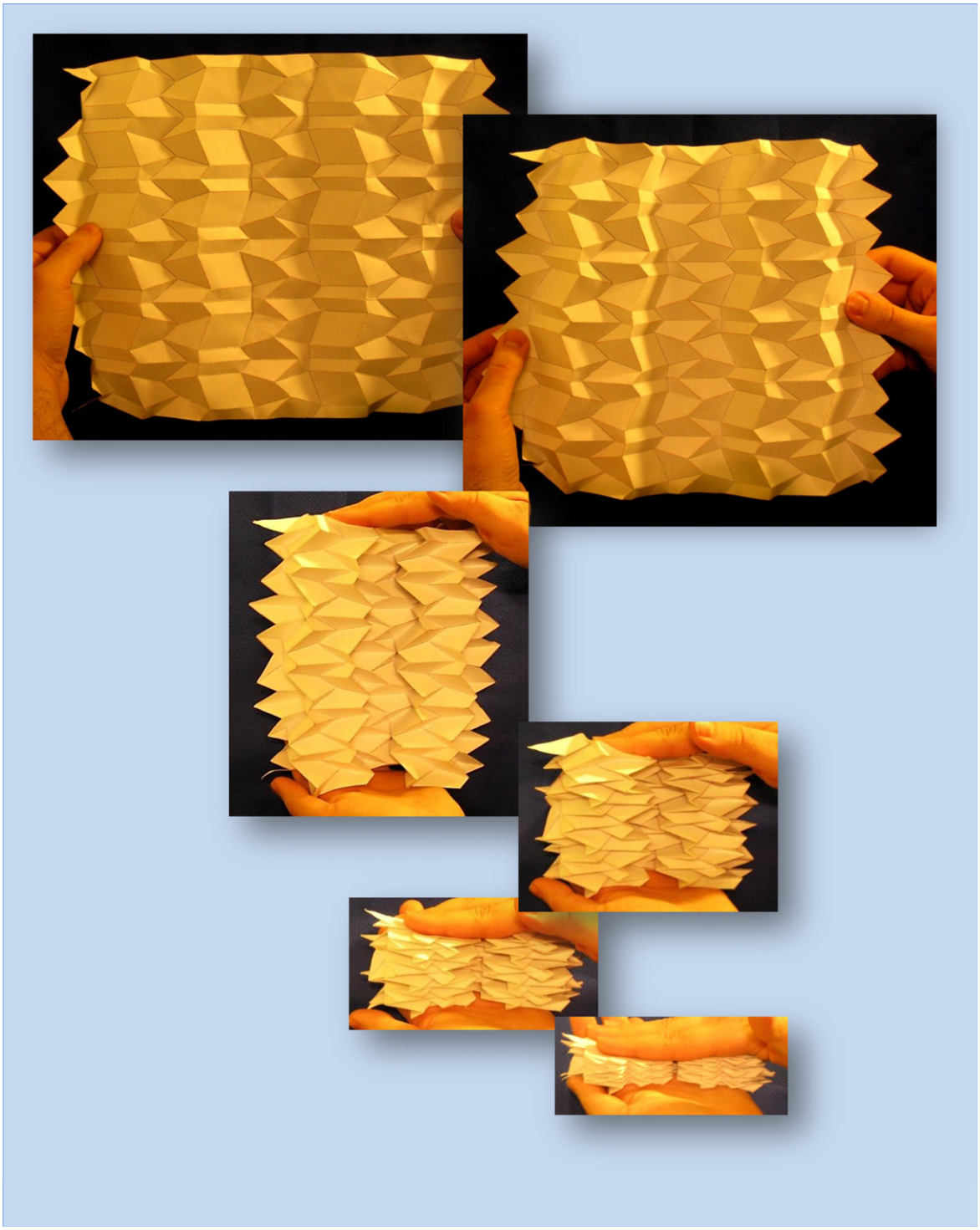

Figure 16. The folding process of a cardboard model of the fold pattern depicted in the previous figure [13].

of the unit cell is located on the midpoint of a side of a parallelogram facet, or on the centroid of it. The two different types of $pmg_{m,n}$ unit cells depending on whether n is even, i.e. $n = 2q$, or odd, i.e. $n = 2q - 1$, where q is a natural number, are presented in [10]. In either case, there are $n \times p$ distinct orbits of nodes associated with the unit cell, shown as $A_{i,j}$, where $1 \leqslant i \leqslant p$ and $1 \leqslant j \leqslant n$. These orbits of nodes are listed in the following matrix:

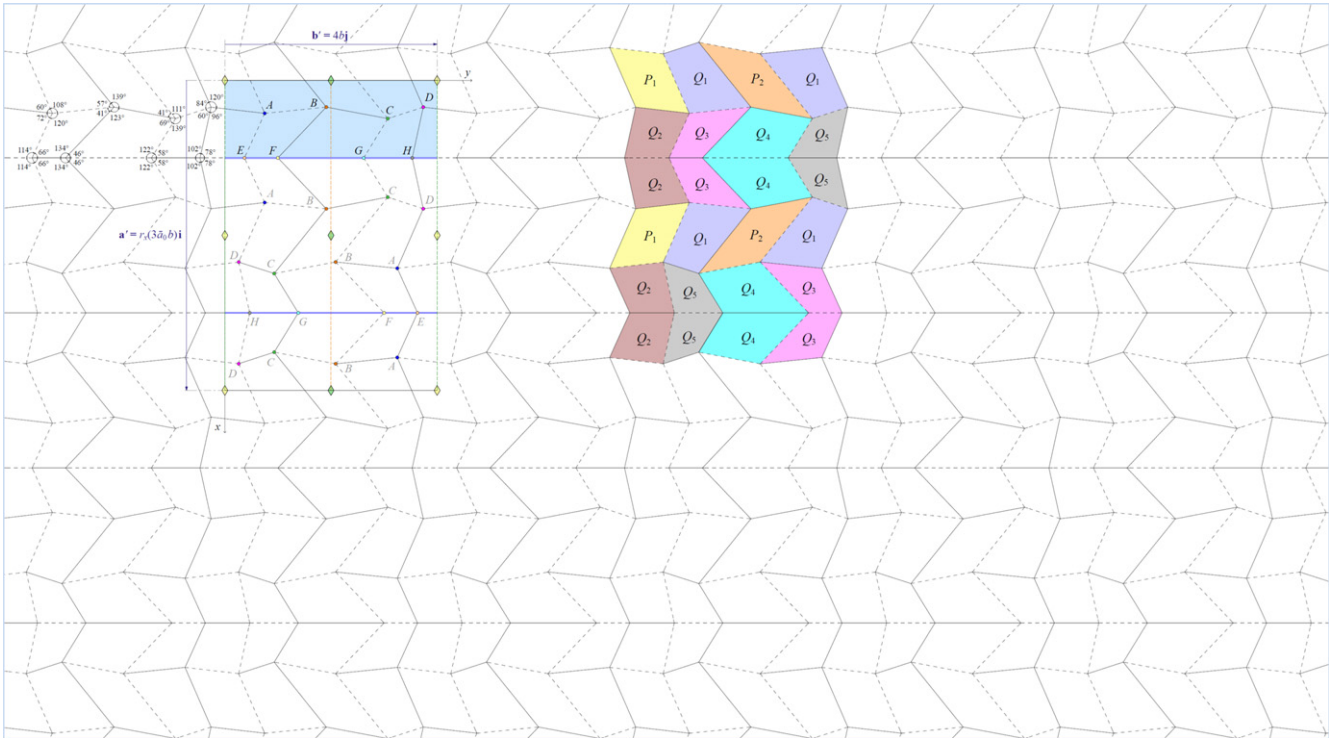

Figure 17. An example for a flat-foldable $pmg^{+}_{6,4}$ variation of the Miura-ori. It consists of five different starting convex quadrilaterals, shown as Q_1, Q_2, Q_3, Q_4 and Q_5, as well as two different parallelograms P_1 and P_2. Solid lines show mountain fold lines, while dashed lines represent valley fold lines.

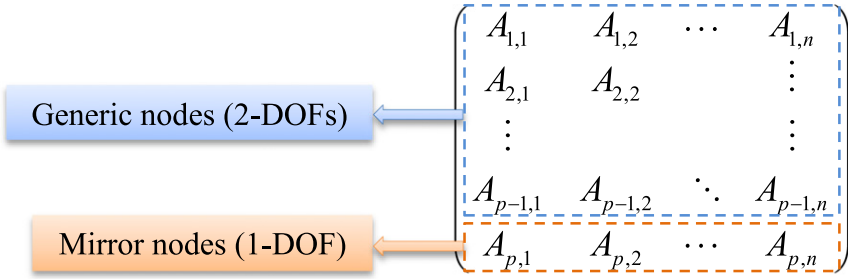

As in every *pmg* symmetry group, there is a degree of freedom for the aspect ratio of the unit cell. The first $p-1$ rows of nodes in the matrix are generic nodes, in which there are two degrees of freedom for each node, providing us with $2n(p-1)$ degrees of freedom. The pth row contains merely mirror nodes, each of them having one degree of freedom, giving us n degrees of freedom. In total, the number of degrees of freedom of the pattern is as follows:

$$\text{Number of DOFs} = \underbrace{1}_{\text{Aspect ratio}} + \underbrace{2n(p-1)}_{\text{Generic nodes}} + \underbrace{n}_{\text{Mirror nodes}} = n(2p-1)+1.$$

Noting that there are $n(p-1)$ flat-foldability equations associated with the $n(p-1)$ generic nodes in the pattern, we conclude:

$$\text{Number of DOFs} - \text{number of equations} = (n(2p-1)+1) - n(p-1) = np+1.$$

Although increasing the size of the unit cell provides us with more degrees of freedom to make design variations on the original pattern, it decreases the number of constraints on a typical quadrilateral within the pattern, making variations with larger m and n less interesting from a symmetry viewpoint.

Figure 15 depicts a $pmg_{6,3}$ variation of the Miura-ori which consists of four distinct starting quadrilaterals as well as a single starting parallelogram. The folding process of this pattern is represented in figure 16 using a cardboard model.

We have shown that, in a $pmg_{m,n}$ variation of the Miura-ori, where $m=2(2p—1)$, the following statements are valid (p and q are natural numbers).

- If n is even, i.e. $n=2q$, there are $q(2p-1)$ distinct convex quadrilaterals in the fold pattern. In the case $m=2$, i.e. $p=1$, all the convex quadrilaterals must be trapezoids.
- If n is odd, i.e. $n=2q-1$, there are $q(2p-1)-p$ distinct convex quadrilaterals in the fold pattern in addition to a single parallelogram. In the case $m=2$, i.e. $p=1$, all the convex quadrilaterals must be trapezoids. In the case $m=2$, i.e. $p=1$, and $n=1$, i.e. $q=1$, the pattern is the Miura-ori which consists of a single parallelogram.

Starting from the alternative standard unit cell, S^+, illustrated in figure 1, we study the alternative $m\times n$ isomorphic variation of the Miura-ori, where $m=2(2p-1)$, and n and p are natural numbers. As described earlier, for n odd, i.e. $n=2q-1$, where q is a natural number, the $pmg^+_{m,n}$ variation of the Miura-ori is the same as the $pmg_{m,n}$ variation studied earlier. In contrast, for n even, $pmg_{m,n}$ and $pmg^+_{m,n}$ are different patterns.

A $pmg^+_{m,2q}$ unit cell is presented in [10]. The details of the degrees of freedom for $pmg^+_{m,2q}$ are similar to the $pmg_{m,2q}$ variation discussed earlier. We have shown that, in a $pmg^+_{m,n}$ variation of the Miura-ori, where $m=2(2p-1)$, the following statements are valid (p and q are natural numbers).

- If n is odd, i.e. $n=2q-1$, the pattern is the same as the $pmg_{m,n}$ variation.
- If n is even, i.e. $n=2q$, there are $q(2p-1)-1$ distinct convex quadrilaterals in the fold pattern in addition to two distinct parallelograms.

Figure 17 depicts a $pmg^+_{6,4}$ variation of the Miura-ori which consists of five distinct starting quadrilaterals as well as two distinct starting parallelograms.

3. Conclusions

Starting with the Miura fold pattern which is a flat-foldable *pmg* wallpaper pattern, we generalized the fold pattern by systematic unit cell enlargements, while at the same time preserving the wallpaper group. We designed and developed flat-foldable isomorphic symmetric descendants for the Miura-ori with a variety of quadrilateral facets, which are either globally planar, or globally curved, while the Miura-ori is a globally planar pattern based on a single starting parallelogram facet. Future research can go beyond generalizing the Miura-ori while preserving its symmetry group, but may include variations of this pattern which have different symmetry groups.

References

[1] Miura K 2006 The science of Miura-ori: a review *4OSME: 4th Int. Conf. on Origami in Science, Mathematics, and Education (Pasadena, CA)*

[2] Hahn T 2005 International tables for crystallography vol A *Space-Group Symmetry* (New York: Springer)

[3] Schwarzenberger R L E 1974 The 17 plane symmetry groups *Math. Gaz.* **58** 123–31

[4] Schattschneider D 1978 The plane symmetry groups: their recognition and notation *Am. Math. Mon.* **85** 439–50

[5] Tachi T 2009 Generalization of rigid-foldable quadrilateral-mesh origami *IASS: Proc. Int. Association for Shell and Spatial Structures (Valencia, Spain)*

[6] Sareh P and Guest S D 2012 Tessellating variations on the Miura fold pattern *IASS: Proc. Int. Association for Shell and Spatial Structures (Seoul, South Korea)*

[7] Sareh P and Guest S D 2015 A framework for the symmetric generalisation of the Miura-ori *Int. J. Space Struct., Spec. Issue Folds Struct.* at press

[8] Radaelli P G 2011 *Symmetry in Crystallography: Understanding the International Tables* (Oxford: Oxford University Press)

[9] Demaine E D and O'Rourke J 2007 *Geometric Folding Algorithms: Linkages, Origami, Polyhedra* (Cambridge: Cambridge University Press)

[10] Sareh P 2014 Symmetric descendants of the Miura-ori *PhD Dissertation* Engineering Department, University of Cambridge, UK

[11] Tachi T 2013 'Freeform Origami' (online) (www.tsg.ne.jp/TT/software/)

[12] Sareh P and Guest S D 2013 Minimal isomorphic symmetric variations on the miura fold pattern *Transformables 2013: Proc. 1st Int. Conf. on Transformable Architecture (Seville, Spain)*

[13] Sareh P and Guest S D 2014 Designing symmetric derivatives of the Miura-ori *Advances in Architectural Geometry* (London: Springer)